Book Chapter

An Approach for Elliptical Trajectory Planning with Vertical Straight Line Segments of Pick-and-Place Robot Operation with Height Clearance

Myong Song Choe[1], Kwan Sik Jang[1], Yong Ho Kim[1], Kyong Hyok Kim[1] and Won-Chol Yang[2]*

[1]Faculty of Mechanical Science and Technology, Kim Chaek University of Technology, Democratic People's Republic of Korea
[2]Faculty of Materials Science and Technology, Kim Chaek University of Technology, Democratic People's Republic of Korea

***Corresponding Author:** Won-Chol Yang, Faculty of Materials Science and Technology, Kim Chaek University of Technology, Pyongyang, Democratic People's Republic of Korea

Published **August 14, 2023**

This Book Chapter is a republication of an article published by Won-Chol Yang, et al. at Mathematical Problems in Engineering in June 2023. (Myong Song Choe, Kwan Sik Jang, Yong Ho Kim, Kyong Hyok Kim, Won-Chol Yang. An Approach for Elliptical Trajectory Planning with Vertical Straight Line Segments of Pick-and-Place Robot Operation with Height Clearance. Mathematical Problems in Engineering. Volume 2023, Article ID 7419178, 12 pages. https://doi.org/10.1155/2023/7419178)

How to cite this book chapter: Myong Song Choe, Kwan Sik Jang, Yong Ho Kim, Kyong Hyok Kim, Won-Chol Yang. An Approach for Elliptical Trajectory Planning with Vertical Straight Line Segments of Pick-and-Place Robot Operation with

Height Clearance. In: Mohamed Ali Hajjaji, editor. Prime Archives in Engineering. Hyderabad, India: Vide Leaf. 2023.

Data Availability: All data that support the findings of this study are included within this article.

Conflicts of Interests: The authors declare that they have no conflicts of interest.

Acknowledgment: The authors received no financial support for the research, authorship and/or publication of this article.

Abstract

This paper deals with elliptical trajectory planning with vertical straight-line segments for pick-and-place robot operation with height clearance. It is significant for trajectory planning for the pick-and-place operation with the different height clearance between the picking point and placing point, or with the height clearance for picking and placing the product in the box. In this paper, we propose an optimal asymmetric bisected elliptical path with two vertical straight line segments and a method to generate motion profile suited to geometry of the optimal asymmetric bisected elliptical path based on radius of curvature. The simulation result demonstrates that the proposed trajectory planning approach enables to reduce workspace and cycle period of pick-and-place operation by minimizing the length and height of the path, and guarantees continuity and smoothness of velocity, acceleration and jerk, and results in smoothness of working action of robot actuators.

Keywords

Pick-and-Place Robot; Trajectory Planning; Elliptical Path; Height Clearance; Motion Profile

Introduction

Trajectory planning is one of the most important problems in robotics. It refers to generate position commands, velocity and acceleration of all degrees of freedom of the robot [1]. It involves establishing the movement of a manipulator from the initial position to the final position and defining the geometric path and the motion law [2]. The capability and efficiency of high-speed pick-and-place parallel robots requires an effective trajectory planning for taking an excellent performance from the viewpoint of smoother joint torque, lower residual vibration and shorter cycle time [3]. The pick-and-place trajectory planning problem is finding a smooth and continuous trajectory from a starting position to a desired terminal position within the workspace of the robot.

Many studies have been conducted for effective trajectory planning of robot. Gosselin et al. [4] used a ninth-order polynomial for a single motion profile to guarantee C3-continuity by inserting a lift-off and a set-down point. Piazzi and Visioli [5] conducted the optimization of global minimum-jerk trajectory planning of robot manipulators using interval analysis. Constantinescu et al. [6] proposed a method for minimum time trajectory planning subject to the limits imposed upon the joint torques and their first derivatives. Chettibi et al. [7] proposed minimum cost trajectory planning algorithm for robotic manipulators using sequential quadratic programming method. Gasparetto et al. [8] used quintic B-spline for the interpolation to generate smooth joint trajectories. Gasparetto et al. [9] proposed time-jerk optimal planning method for robot trajectories by using sequential quadratic programming techniques in order to get the optimal trajectory. Gauthier et al. [10] used Lamé curves with G^2-continuity at the square corners linked the vertical segment and horizontal one, and applied '4-5-6-7 polynomial' with C^3-continuity as the motion profile. The trajectory was generated to

minimize the root of mean square of the time-derivative of the kinetic energy per unit mass of the payload. Saravanan et al. [11] proposed evolutional theory based method for optimal trajectory planning using uniform cubic B-splines. Ramabalan et al. [12] proposed two efficient evolutionary optimization techniques such as NSGA-II and MODE for doing off-line tridimensional optimal trajectory planning of the industrial robot manipulators in the presence of fixed obstacles. Gasparetto et al. [13] proposed an algorithm for optimal smooth trajectory planning by minimizing, subject to limits on joint velocity, acceleration and jerk, a weighted sum of the integral of joint jerk squared and the total cycle time. Rossi et al. [2] proposed a method for the robot trajectory planning, which consisted in controlling a manipulator by assigning not only the way points on the path but also the geometrical tangent of the desired path shape at each of those points. Liu et al. [14] proposed time-optimal and jerk-continuous trajectory planning approach by combining the spline interpolating in Cartesian space and B-spline interpolating in joint space to gain a high smooth tracking performance in the practical motion task. Wang et al. [15] proposed the robot trajectory planning model of a tower crane welding robot was established based on a Bezier curve method according to the time optimal method. Jahanpour et al. [16] proposed a novel trajectory planning scheme for parallel machining robot with 4 (UPS)-PU mechanism by using NURBS curves. Kucuk [17] proposed algorithm for optimal trajectory generation to generate minimum-time smooth motion trajectories for serial and parallel manipulators. Masey et al. [18] proposed bisected ellipse as the geometric path such that the arc length along the path was approximated as the linear function of two normalized parameters including any specified durations of constant velocity or degree of asymmetry. Wu et al. [19] proposed the multi-objective design optimization method of a parallel Schonflies-motion robot. Zhang et al. [20] studied on the trajectory planning and optimization for a Par4 parallel robot based on energy consumption in high-speed picking and placing. They used Lamé curve in the trajectory planning, and introduced asymmetric displacement planning based on the quintic and sextic polynomial motion laws to minimize the total mechanical energy consumption of the driving joints. They used Grey Wolf

Optimizer for optimizing the Lamé curve parameters. Wang et al. [21] proposed a smooth point-to-point trajectory planning based on high-order polynomial curve for industrial robots with kinematical constraints. Wu et al. [22] proposed a novel point-to-point trajectory planning algorithm based on a locally asymmetrical jerk motion profile for the time-optimal and smooth joint trajectories of industrial robots. Wu et al. [23] proposed a multi-objective (time and jerk) integrated trajectory planning method based on improved butterfly optimization algorithm to improve the dynamic performance of the Delta parallel pickup robot in high-speed pick-and-place processes. The pick-and place trajectory of the robot was constructed using NURBS curves. Liu et al. [24] proposed four-phase pick-and-place trajectory planning scheme based on S-shaped acceleration/ deceleration algorithm and quintic polynomial trajectory planning method of the cable-based gangue-sorting robot in the operation space.

The most of the previous works for trajectory planning mainly focused to generating the smoother path and motion profile for the purpose of smoother joint torque, lower residual vibration, jerk continuity and minimization, minimization of cycle period and mechanical energy. However, the previous works lack in considering the minimization of the workspace, and especially, their equations of velocity and acceleration/deceleration contain little information of the path, and therefore the equations are no direct related to the geometry of the generated path. It is desirable that the velocity and acceleration/deceleration equations reflect the information of the path and are direct related to the path. On the other hand, the paths and motion profiles are pre-calculated in the most of the previous methods. It may be difficult to calculate those tasks during one cycle period of pick-and-place operation in real-time by robot controller. It is not suitable to the high-speed pick-and-place operation of the moving objects on belts and it becomes the practical limitation of the use of the previous trajectory planning methods.

To solve these problems, this paper focuses on developing the asymmetric bisect elliptical trajectory planning with minimum workspace and trajectory planning approach suited to geometry

of the path in real-time for pick-and-place operation in which both the picking points and placing points are changed randomly in the workspace.

The rest of this paper is organized as follows. In subsection 2.1, we propose an optimal asymmetric bisect elliptical path with two vertical straight line segments. In subsection 2.2, we propose a method to generate optimal asymmetric bisected elliptical path. In subsection 2.3, we propose a method to generate the motion profile suited to geometry of the optimal elliptical path based on radius of curvature. In section 3, we describe the simulation test results using the proposed method to demonstrate the effectiveness of the proposed method.

Methods

Optimal Asymmetric Bisected Elliptical Path with Two Vertical Straight Line Segments

In this subsection, we propose an optimal asymmetric bisect elliptical path with two vertical straight line segments.
Let P_1 and P_2 be the initial and final points of the end effector in a pick-and-place operation in the reference frame O–xyz. (Figure 1) The pick-and-place path consists of two vertical straight line segments and asymmetric bisected ellipse tangent to these two line segments, where φ represents the angle between x-axis and the major axis of the ellipse, and $T_1(-l, -h)$ and $T_2(l, h)$ are two tangent points of the bisected ellipse and two vertical line segments.

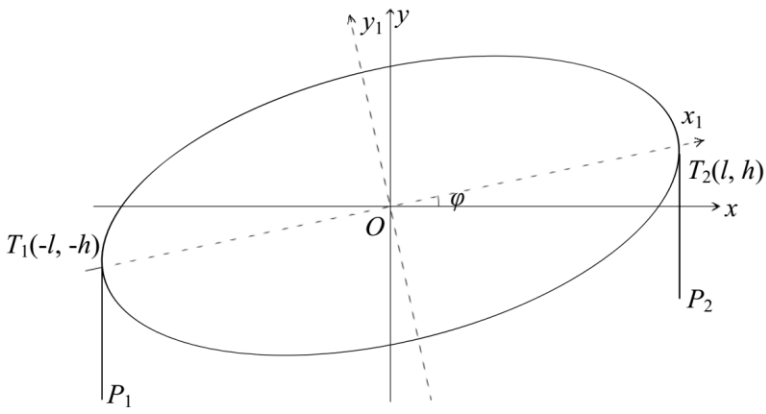

Figure 1: Optimal asymmetric bisected elliptical path with two vertical straight line segments.

In the local frame O–$x_1y_1z_1$, the equation of the ellipse is as follows:

$$\frac{x_1^2}{a^2}+\frac{y_1^2}{b^2}=1, \tag{1}$$

where a and b are the semi-major radius and semi-minor radius of the ellipse, respectively.

The relationship between the reference frame O–xyz and the local frame O–$x_1y_1z_1$ can be represented as equation (2).

$$\begin{bmatrix} x_1 \\ y_1 \end{bmatrix}=\begin{bmatrix} \cos\varphi & \sin\varphi \\ -\sin\varphi & \cos\varphi \end{bmatrix}\begin{bmatrix} x \\ y \end{bmatrix}=\begin{bmatrix} x\cos\varphi+y\sin\varphi \\ -x\sin\varphi+y\cos\varphi \end{bmatrix}, \tag{2a}$$

$$\begin{bmatrix} x \\ y \end{bmatrix}=\begin{bmatrix} \cos\varphi & -\sin\varphi \\ \sin\varphi & \cos\varphi \end{bmatrix}\begin{bmatrix} x_1 \\ y_1 \end{bmatrix}=\begin{bmatrix} x_1\cos\varphi-y_1\sin\varphi \\ x_1\sin\varphi+y_1\cos\varphi \end{bmatrix}. \tag{2b}$$

By substituting equation (2a) into equation (1), we have

$$\frac{(x\cos\varphi+y\sin\varphi)^2}{a^2}+\frac{(-x\sin\varphi+y\cos\varphi)^2}{b^2}=1,$$

$\frac{1}{a^2}(\cos^2\varphi\cdot x^2+\sin 2\varphi\cdot xy+\sin^2\varphi\cdot y^2)+\frac{1}{b^2}(\sin^2\varphi\cdot x^2-\sin 2\varphi\cdot xy+\cos^2\varphi\cdot y^2)=1$,

$$(\frac{\cos^2\varphi}{a^2}+\frac{\sin^2\varphi}{b^2})\cdot x^2+(\frac{\sin 2\varphi}{a^2}-\frac{\sin 2\varphi}{b^2})\cdot xy+(\frac{\sin^2\varphi}{a^2}+\frac{\cos^2\varphi}{b^2})\cdot y^2=1. \quad (3)$$

Above equation can be expressed as follows:

$$Ax^2+Bxy+Cy^2=1, \quad (4)$$

Where

$$A=\frac{\cos^2\varphi}{a^2}+\frac{\sin^2\varphi}{b^2}, B=\frac{\sin 2\varphi}{a^2}-\frac{\sin 2\varphi}{b^2}, C=\frac{\sin^2\varphi}{a^2}+\frac{\cos^2\varphi}{b^2}. \quad (5)$$

Since two points $T_1(-l, -h)$ and $T_2(l, h)$ are located on the ellipse,

$$Al^2+Blh+Ch^2=1. \quad (6)$$

By differentiating both sides of the equation (3) on x, we have

$$2Ax+By+Bxy'+2Cyy'=0. \quad (7)$$

Hence

$$y'=-\frac{2Ax+By}{Bx+2Cy}. \quad (8)$$

Since

$$y'\Big|_{x=\pm l}=\infty. \quad (9)$$

at the points $T_1(-l, -h)$ and $T_2(l, h)$, we have

$$Bl+2Ch=0, \text{ that is, } Bl=-2Ch. \quad (10)$$

By Substituting the equation (8) into the equation (3),

$$Al^2-2Ch^2+Ch^2=1, \text{ that is } Al^2-Ch^2=1. \quad (11)$$

From the equation (8),

$$\left(\frac{\sin 2\varphi}{a^2}-\frac{\sin 2\varphi}{b^2}\right)l=-2\left(\frac{\sin^2\varphi}{a^2}+\frac{\cos^2\varphi}{b^2}\right)h. \quad (12)$$

By multiplying above equation by a^2b^2, we have

$$\left(l\sin 2\varphi+2h\sin^2\varphi\right)b^2=\left(l\sin 2\varphi-2h\cos^2\varphi\right)a^2. \quad (13)$$

Above equation can be expressed as follows:

$Db^2=Ea^2$, that is, $b^2=Ea^2/D$, (14)

where

$$D=l\sin 2\varphi+2h\sin^2\varphi, E=l\sin 2\varphi-2h\cos^2\varphi. \quad (15)$$

From the equation (9),

$$(\frac{\cos^2\varphi}{a^2}+\frac{\sin^2\varphi}{b^2})\cdot l^2-(\frac{\sin^2\varphi}{a^2}+\frac{\cos^2\varphi}{b^2})\cdot h^2=1. \quad (16)$$

By multiplying above equation by a^2b^2, we have

$$\left(l^2\sin^2\varphi-h^2\cos^2\varphi\right)a^2+\left(l^2\cos^2\varphi-h^2\sin^2\varphi\right)b^2=a^2b^2. \quad (17)$$

Above equation can be expressed as follows:

$Fa^2+Gb^2= a^2b^2$, (18)

where

$$F=l^2\sin^2\varphi-h^2\cos^2\varphi, G=l^2\cos^2\varphi-h^2\sin^2\varphi. \quad (19)$$

By substituting the equation (10) into the equation (11),

$Fa^2+GEa^2/D = a^2Ea^2/D$. (20)

From this equation, we have

$a^2=DF/E+G$. (21)

By substituting the equation (12) into the equation (10),

$b^2=E/D\cdot(DF/E+G)$, (22)

that is,

$b^2= F+EG/D$. (23)

Since D, E, F and G are the functions of φ, it is sure that a and b are also the functions of φ, that is, $a= a(\varphi)$ and $b= b(\varphi)$ from the equations (12) and (13). Hence, A, B and C are also the functions of φ, that is, $A= A(\varphi)$, $B= B(\varphi)$ and $C= C(\varphi)$ in the equation (4).

Therefore, when the angle φ is given, the only ellipse satifying the equations (5) and (7) is determined as follows:

$A(\varphi)\cdot x^2+B(\varphi)\cdot xy+C(\varphi)\cdot y^2=1$, (24)

Where

$$A(\varphi)=\frac{\cos^2\varphi}{a^2(\varphi)}+\frac{\sin^2\varphi}{b^2(\varphi)}, B(\varphi)=\frac{\sin 2\varphi}{a^2(\varphi)}-\frac{\sin 2\varphi}{b^2(\varphi)}, C(\varphi)=\frac{\sin^2\varphi}{a^2(\varphi)}+\frac{\cos^2\varphi}{b^2(\varphi)}. \quad (25)$$

We have to determine the optimal angle φ^* so that the length of the asymmetric bisected elliptical path is minimum.

The length of the asymmetric bisected elliptical path is equal to the perimeter length of the semi-ellipse with semi-major radius a and semi-minor radius b.

In general, it is impossible to analytically calculate the perimeter length of the semi-ellipse and it can be calculated by numerical integration method. In order to calculate it, we develop its approximate formula.

Commonly, the following inequality is satisfied about the perimeter length L of the semi-ellipse:

$$L_l = \pi(a+b)/2 < L < L_u = \frac{\pi}{\sqrt{2}}\sqrt{a^2+b^2}\ . \tag{26}$$

Therefore, we can derive the approximate formula for the perimeter length of the semi-ellipse as follows:

$$L \approx L_m = \frac{1}{2}(L_l + L_u) = \frac{1}{2}\left[\pi(a+b)/2 + \frac{\pi}{\sqrt{2}}\sqrt{a^2+b^2}\right]. \tag{27}$$

To verify its availability, varying a from 5 to 20 and b from 2 to 20, we calculated the perimeter lengths of the semi-ellipse by using both the numerical integration method and the equation (16), and then evaluate their mean absolute error and mean relative error in MATLAB. As a result, the mean absolute error was 0.078, and the mean relative error was 0.231%. It demonstrates that the equation (16) could be used to calculate the perimeter length of the semi-ellipse, approximately.

Therefore, the optimal asymmetric bisected elliptical path could be determined as follows.

Given the values of l and h, it is the asymmetric bisected elliptical path with the optimal angle φ^* so that the following objective function has the minimum value.

$$L(\varphi) \approx \frac{1}{2}\left[\pi(a(\varphi)+b(\varphi))/2 + \frac{\pi}{\sqrt{2}}\sqrt{a^2(\varphi)+b^2(\varphi)}\right]. \tag{28}$$

To intuitively demonstrate the behavior of the objective function (17), we calculated the perimeter length $L(\varphi)$of the elliptical path according to angle φ using the equation (17) by varying the angle φ from the critical angle $\left[\frac{180}{\pi}\arctan(\frac{h}{l})\right]°$ to 60° step 1°, and plotted the graph in case of l =0.150 and h=0.025. The result is shown in Figure 2. From Figure 2, we can know that the smaller the angle φ is, the shorter the elliptical path is. In this case, the

optimal angle with minimum length of the elliptical path is $\varphi^*=10°$.

By analyzing the equation (17) and Figure 2, we can know that the function is a monotonically increasing curve for angle φ.

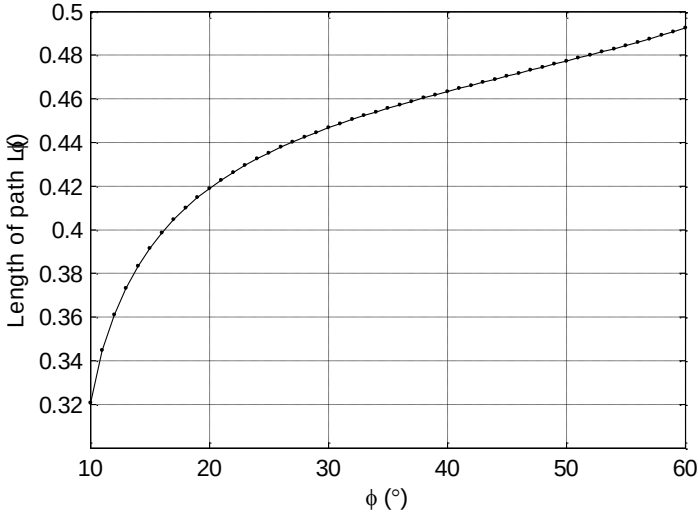

Figure 2: Perimeter length of the elliptical path according to angle φ (°)

Therefore, we can determine the optimal angle φ^* with minimum length of elliptical path as the critical angle using the following equation:

$$\varphi^*=\left[\frac{180}{\pi}\arctan(\frac{h}{l})\right]\cdot\frac{\pi}{180}, \tag{29}$$

where $[x]$ denotes the ceiling number of x.

The optimal semi-major radius a^* and semi-minor radius b^* are calculated using the following equations:

$$a^{*2}=D^*F^*/E^*+G^*, \tag{30}$$

$$b^{*2}=E^*/D^*\cdot(D^*F^*/E^*+G^*), \tag{31}$$

where

$$\begin{aligned} D^* &= l\sin 2\varphi^* + 2h\sin^2\varphi^*, \\ E^* &= l\sin 2\varphi^* - 2h\cos^2\varphi^*, \\ F^* &= l^2\sin^2\varphi^* - h^2\cos^2\varphi^*, \\ G^* &= l^2\cos^2\varphi^* - h^2\sin^2\varphi^*. \end{aligned} \tag{32}$$

Next, we determine the top point and its height of the optimal asymmetric bisected elliptical path.

On the top point of the optimal elliptical path, its derivative y' should be 0.

From the equation (6), the following equation should be satisfied:

$$2Ax+By=0. \tag{33}$$

By considering the equation (2b),

$$\begin{cases} x = x_1\cos\varphi - y_1\sin\varphi = a\cos\varphi\cos\theta - b\sin\varphi\sin\theta \\ y = x_1\sin\varphi + y_1\cos\varphi = a\sin\varphi\cos\theta + b\cos\varphi\sin\theta \end{cases}. \tag{34}$$

By substituting above equation into the equation (21), we have

$$\begin{aligned} &2A(a\cos\varphi\cos\theta - b\sin\varphi\sin\theta) + B(a\sin\varphi\cos\theta + b\cos\varphi\sin\theta) = 0, \\ &(2Aa\cos\varphi + Ba\sin\varphi)\cos\theta - (2Ab\sin\varphi - Bb\cos\varphi)\sin\theta = 0, \\ &\tan\theta = \frac{\sin\theta}{\cos\theta} = \frac{2Aa\cos\varphi + Ba\sin\varphi}{2Ab\sin\varphi - Bb\cos\varphi}. \end{aligned} \tag{35}$$

Therefore, the polar angle according to the top point is as follows:

$$\theta^* = \arctan\left(\frac{2Aa\cos\varphi + Ba\sin\varphi}{2Ab\sin\varphi - Bb\cos\varphi}\right). \tag{36}$$

The top point T (x^*, y^*) is as follows:

$$\begin{cases} x^* = a\cos\varphi\cos\theta^* - b\sin\varphi\sin\theta^* \\ y^* = a\sin\varphi\cos\theta^* + b\cos\varphi\sin\theta^* \end{cases}. \tag{37}$$

Therefore, the height of the top point is as follows:

$$H^* = |a\sin\varphi\cos\theta^* + b\cos\varphi\sin\theta^*|. \tag{38}$$

The height of top point determines the working space of the robot. The lower the top point is, the smaller the working space is.

Method to Generate Optimal Asymmetric Bisected Elliptical Path

In this subsection, we propose a method to generate optimal asymmetric bisected elliptical path.

The main steps to generate the optimal asymmetric bisected elliptical path are as follows:

Step 1: Determine the polar angles θ_{T1} and θ_{T2} corresponding to the tangent points T_1 and T_2 on the elliptical path in the local frame O–$x_1y_1z_1$.

The polar angle θ_{T2} is calculated as follows:

Consider the equation (2a):

$$\begin{bmatrix} x_1 \\ y_1 \end{bmatrix} = \begin{bmatrix} x\cos\varphi + y\sin\varphi \\ -x\sin\varphi + y\cos\varphi \end{bmatrix}, \tag{39}$$

and the parametric equation of the ellipse:

$$\begin{cases} x_1 = a\cos\theta \\ y_1 = b\sin\theta \end{cases}, \tag{40}$$

where the parameter θ is polar angle in the local frame O–$x_1y_1z_1$.

Since the coordinates of the last tangent point of the elliptical path is $T_2(l, h)$, by substituting $x= l$ and $y= h$ into $y_1= -x\sin\varphi^* + y\cos\varphi^*= b\sin\theta$, we have $-l\sin\varphi^*+ h\cos\varphi^*= b\sin\theta_{T2}$. From this equation, θ_{T2} is calculated as follows:

$$\theta_{T2}= \arcsin[(-l\sin\varphi^* + h\cos\varphi^*)/b]. \tag{41}$$

θ_{T1} of the first tangent point $T_1(-l, -h)$ of the elliptical path is calculated as follows:

$$\theta_{T1}= \theta_{T2}+ \pi. \tag{42}$$

Step 2: Calculate the coordinates $\{(x_p(\theta), y_p(\theta)); \theta_{T2}\leq\theta\leq\theta_{T1}\}$ of the points on the elliptical path as follows:

$$\begin{cases} x_p(\theta) = a\cos\varphi^*\cos\theta - b\sin\varphi^*\sin\theta \\ y_p(\theta) = a\sin\varphi^*\cos\theta + b\cos\varphi^*\sin\theta \end{cases}; \ \theta_{T2}\leq\theta\leq\theta_{T1} \tag{43}$$

Step 3: Generate the optimal asymmetric bisected elliptical path using the points $\{(x_p(\theta), y_p(\theta)); \theta_{T2}\leq\theta\leq\theta_{T1}\}$ in the reference frame O–xyz.

Method to Generate Motion Profile Suited to Geometry of Optimal Elliptical Path based on Radius of Curvature

In this subsection, we propose a method to generate the motion profile suited to geometry of the optimal elliptical path based on radius of curvature.

The parametric equation of the ellipse is as follow:

$$\begin{cases} x = x(\theta) = a\cos\varphi\cos\theta - b\sin\varphi\sin\theta \\ y = y(\theta) = a\sin\varphi\cos\theta + b\cos\varphi\sin\theta \end{cases}. \tag{44}$$

From the equation (29), we have

$$\begin{cases} x'(\theta) = -a\cos\varphi\sin\theta - b\sin\varphi\cos\theta \\ y'(\theta) = -a\sin\varphi\sin\theta + b\cos\varphi\cos\theta \end{cases}, \tag{45}$$

$$\begin{cases} x''(\theta) = -a\cos\varphi\cos\theta + b\sin\varphi\sin\theta \\ y''(\theta) = -a\sin\varphi\cos\theta - b\cos\varphi\sin\theta \end{cases}. \tag{46}$$

The formula of curvature is as follows:

$$K = \frac{\left|x'(\theta)y''(\theta) - x''(\theta)y'(\theta)\right|}{\left[x'(\theta)^2 + y'(\theta)^2\right]^{3/2}}. \tag{47}$$

Substitute the equations (30) and (31) into (32).
The denominator of the equation (32) is as follows:

$$\begin{aligned} &\left[x'(\theta)^2 + y'(\theta)^2\right]^{3/2} = \left[(-a\cos\varphi\sin\theta - b\sin\varphi\cos\theta)^2 + (-a\sin\varphi\sin\theta + b\cos\varphi\cos\theta)^2\right]^{3/2} \\ &= \left[a^2\cos^2\varphi\sin^2\theta + 2ab\cos\varphi\sin\varphi\sin\theta\cos\theta + b^2\sin^2\varphi\cos^2\theta + \right. \\ &\left. a^2\sin^2\varphi\sin^2\theta - 2ab\cos\varphi\sin\varphi\sin\theta\cos\theta + b^2\cos^2\varphi\cos^2\theta\right]^{3/2} \\ &= (a^2\cdot\sin^2\theta + b^2\cdot\cos^2\theta)^{3/2}. \end{aligned} \tag{48}$$

The numerator of the equation (32) is as follows:

$$\begin{aligned} &\left|x'(\theta)y''(\theta) - x''(\theta)y'(\theta)\right| = \\ &= \left|(a^2\sin\varphi\cos\varphi\sin\theta\cos\theta + ab\cos^2\varphi\sin^2\theta + ab\sin^2\varphi\cos^2\theta + b^2\sin\varphi\cos\varphi\sin\theta\cos\theta) - \right. \\ &\left. -(a^2\sin\varphi\cos\varphi\sin\theta\cos\theta - ab\sin^2\varphi\sin^2\theta - ab\cos^2\varphi\cos^2\theta + b^2\sin\varphi\cos\varphi\sin\theta\cos\theta)\right| \\ &= ab\cdot\cos^2\varphi + ab\cdot\sin^2\varphi = ab. \end{aligned} \tag{49}$$

As a result, the curvature is as follows:

$$K = K(\theta) = \frac{ab}{(a^2 \cdot \sin^2\theta + b^2 \cdot \cos^2\theta)^{3/2}}. \quad (50)$$

Therefore, the radius of curvature is as follows:

$$\rho = \rho(\theta) = \frac{1}{K(\theta)} = \frac{(a^2 \cdot \sin^2\theta + b^2 \cdot \cos^2\theta)^{3/2}}{ab}. \quad (51)$$

This becomes a key equation of the proposed method to generate motion profile suited to geometry of the optimal elliptical path. Based on this principle, we propose a method to generate the motion profile suited to geometry of the optimal elliptical path as follows:

Step 1: Calculate the optimal angle (critical angle) φ^* using the equation (18).

Step 2: Calculate the first and last angles θ_{T1} and θ_{T2} using the equations (26) and (27) as follows:

$$\theta_{T2} = \arcsin[(-l\sin\varphi^* + h\cos\varphi^*)/b],\ \theta_{T1} = \theta_{T2} + \pi. \quad (52)$$

Step 3: $i = 1$, $\theta_i = \theta_{T1}$.

Step 4: Calculate the radius of curvature at the point corresponding to the polar angle θ_i using the equation (34) as follows:

$$\rho(\theta_i) = \frac{1}{K(\theta_i)} = \frac{(a^2 \cdot \sin^2\theta_i + b^2 \cdot \cos^2\theta_i)^{3/2}}{ab}. \quad (53)$$

Step 5: Calculate the coordinates (x_i, y_i) of the point corresponding to the polar angle θ_i using the equation (29) as follows:

$$\begin{cases} x_i = a\cos\varphi^*\cos\theta_i - b\sin\varphi^*\sin\theta_i \\ y_i = a\sin\varphi^*\cos\theta_i + b\cos\varphi^*\sin\theta_i \end{cases}. \quad (54)$$

Step 6: Calculate the polar angle variation $\Delta\theta_i = r \bullet \rho(\theta_i)$, where r is the proportionality coefficient. It should be determined by considering that the maximum acceleration satisfies its allowable value according to the features of the robot such as movement capacity.

Step 7: If $\theta_i > \theta_{T2}$ then set $i = i+1$ and $\theta_i = \theta_{i-1} - \Delta\theta_{i-1}$, and go to Step 4 else go to Step 8.

Step 8: $n = i$.

By using this algorithm, we can determine the coordinates $\{(x_i, y_i); i=1, 2,\ldots, n\}$ of the nodes (key points) on the motion profile of the optimal elliptical path in real-time.

The length of the segment on the motion profile is calculated as follows:

$$\Delta s_i = \sqrt{(x_{i+1} - x_i)^2 + (y_{i+1} - y_i)^2} \; ; i=1, 2,\ldots, n\text{-}1. \qquad (55)$$

The motion profiles on two vertical straight line segments P_1T_1 and T_2P_2 should be determined so that the continuity of the motion veleocity and acceraltion satisfy at the tangent points T_1 and T_2, and the motion times of P_1T_1 and T_2P_2 are shortest.

Results and Discussion

To demonstrate the effectiveness of the key equation (34) (equation of radius of curvature) of the proposed method to generate motion profile suited to geometry of the optimal elliptical path, we first plot the graphs of the radius of curvature $\rho(\theta)$, and its first and second derivations $\rho'(\theta)$ and $\rho''(\theta)$ using the equation (34) in case of $a = 0.3$ and $b=0.05$ (Figure 3). The radius of curvature $\rho(\theta)$ is corresponding to the velocity, and its first and second derivations $\rho'(\theta)$ and $\rho''(\theta)$ are corresponding to the acceleration and jerk.

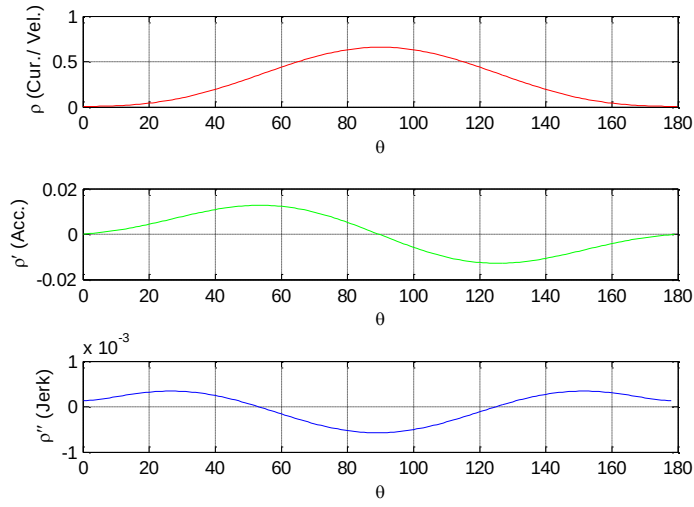

Figure 3: Graphs of the radius of curvature, and its first and second derivations.

From Figure 3, we can intuitively grasp that graphs of the radius of the curvature, and its first and second derivations are bounded, continuous and very smooth. Therefore, the velocities, accelerations and jerks on the generated motion profile are also bounded, continuous and very smooth when we generate the motion profile according to the radius of curvature of the path, and it is reasonable to generate the motion profile according to the magnitude of the radius of curvature of each point on the optimal elliptical path.

To illustrate the proposed method, we next generate the optimal elliptical path and its motion profile when the width of the path is 300 mm and the lift-height of the path is 50 mm.

The simulation scene is shown in Figure 4. In Figure 4, the object is picked from the left box and placed into the right box, and the path consists of vertical line P_1T_1, elliptic curve $\overset{\frown}{T_1T_2}$ and vertical line T_2P_2. In the simulation, we pay attention to the elliptical path.

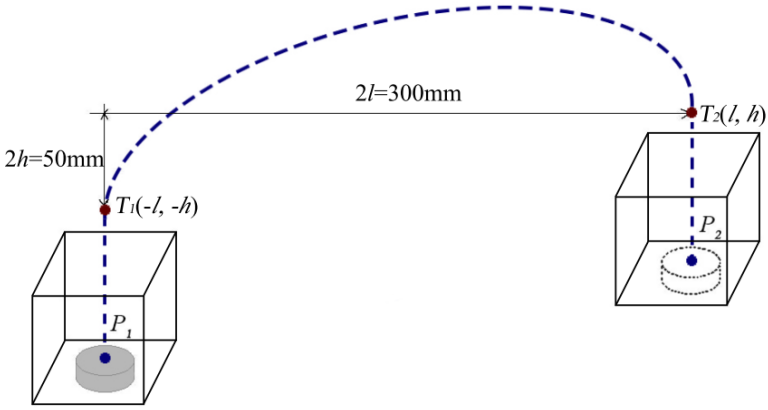

(a)

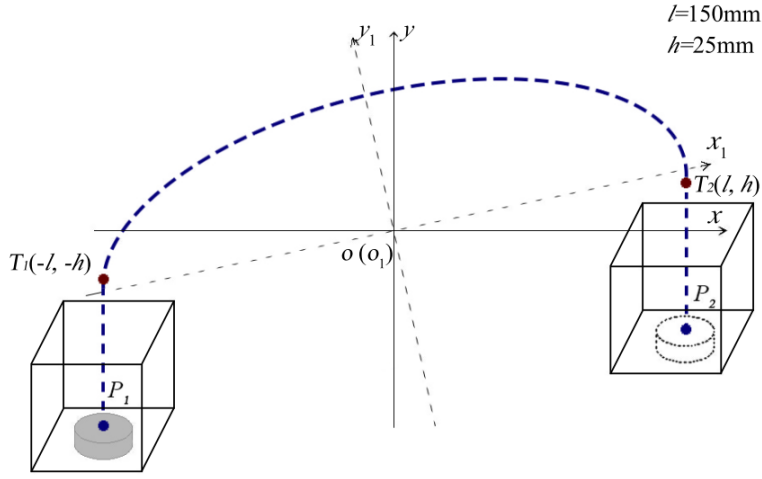

(b)

Figure 4: Simulation scene (a) without coordinate axes, (b) with coordinate axes)

By using the equations (18)–(20), (26) and (27), the optimal angle with minimum length of elliptical path is φ^*= 10, the optimal semi-major radius and semi-minor radius are a^*= 0.15219, b^*= 0.03511, the first and last angles are θ_{T1}= -2.329° and θ_{T2}=177.671°, and the minimum length of the elliptical path

is L^*= 0.32058. By using the equations (24) and (25), the top point of the optimal elliptical path is (0.08617, 0.04352) and the top height is H^*= 0.06852.

In this case, we generate the optimal elliptical path and its motion profile using the generating method of the motion profile suited to geometry of the optimal elliptical path from subsection 2.3. The graphical results are shown in Figures 5–7.

Figure 5 shows the plots of radius of curvature of the optimal elliptical path, displacement, velocity, acceleration and jerk at each knot on the motion profile obtained using the proposed method. (The proportionality coefficient is r= 0.77 in Step 6, subsection 2.3.)

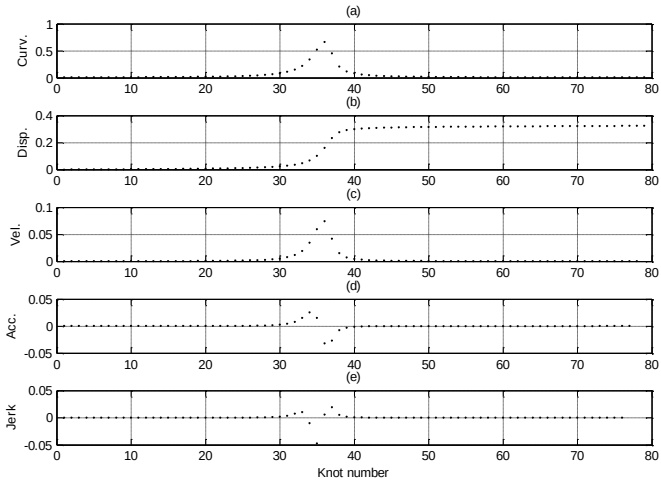

Figure 5: Plots of radius of curvature, displacement, velocity, acceleration and jerk at each knot on the optimal elliptical path: (a) radius of curvature (Curv.), (b) displacement (Disp.), (c) velocity (Vel.), (d) acceleration (Acc.), (e) jerk.

Figure 5 demonstrates that the displacement, velocity, acceleration and jerk are bounded, continuous and smooth. It enables to reduce the fluctuation of velocity, acceleration, jerk of the resulting trajectory. It guarantees the stability of the output torque of actuators and movement of the industrial robot. The proposed elliptical path consists of a single segment, while the

other pick-and-place paths consist of two or more segments. The velocity and acceleration curves of the proposed elliptical path may be smoother than other paths. The elliptical cycle exhibits very smooth and continuous motion curves, and it can reduce the peak joint torques and increase the maximum pick-and-place speed. On the other hand, by the proposed motion profile, the velocity gradually increases from the start point to the top point of the ellipse, and it gradually decreases from the top point to the last point of the ellipse.

Figure 6 shows the optimal elliptical path and its motion profile using the proposed method, where the red and green circles indicate the start and last points, the blue points indicate the nodes (key points) on the motion profile, and the black triangle "Δ" indicates the top point of the optimal elliptical path.

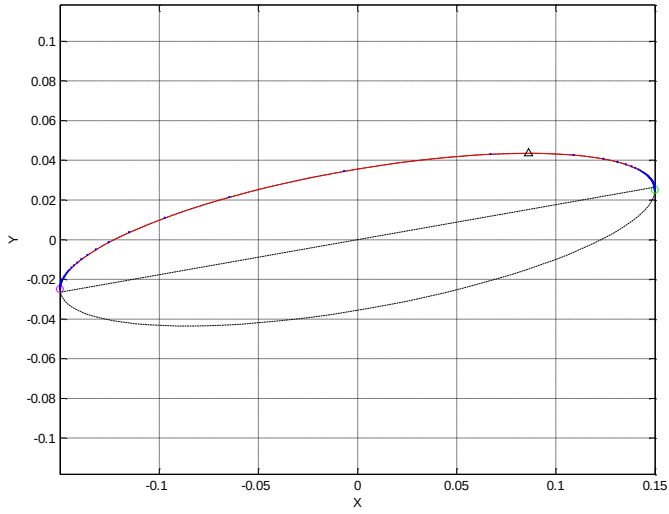

Figure 6: Optimal elliptical path (red curve line) and motion profile (blue points) using the proposed trajectory planning approach.

Figure 6 intuitively demonstrates that the velocity gradually increases from the start point with minimum radius of curvature to the top point of the ellipse with maximum one, and it

gradually decreases from the top point with maximum one to the last point of the ellipse with minimum one.

Figures 4–6 demonstrate that the larger radius of curvature is, the larger the motion displacement, velocity and acceleration are. The velocity of the point with larger radius of curvature is faster than the point with smaller radius of curvature.

Figure 7 shows the displacements of three joint angles α (red solid line), β (green dot-dashed line) and γ (blue dashed line), which are simulated using the proposed trajectory planning method in 3-DOF Delta parallel robot.

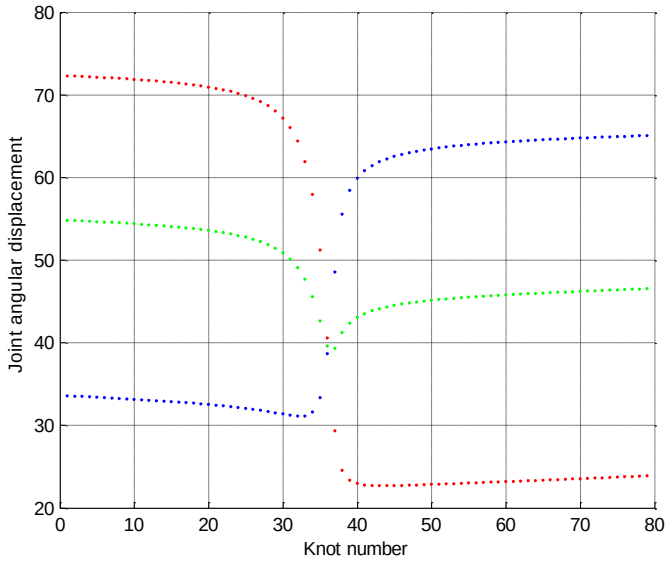

Figure 7: Displacements of joint angles α (red plots), β (green plots) and γ (blue plots).

Figure 7 intuitively demonstrates that the displacements of the joint angles are very smooth and it can enables to reduce the residual vibration of the manipulator when 3-DOF Delta parallel robot conducts the pick-and-place operation using the proposed trajectory planning approach.

To intuitively demonstrate one of the advantages of the proposed method, we compare the length of the proposed optimal asymmetric bisect elliptical path with the lengths of the symmetric bisect elliptical path, Lamé curve with d= 0.05 and e= 0.025, and Lamé curve with d= 0.15 and e= 0.025 when the width of the workspace is 300 mm and the lift-height of the path is 50 mm. The equation of Lamé curve is $\left|u/d\right|^m + \left|v/e\right|^m = 1$.

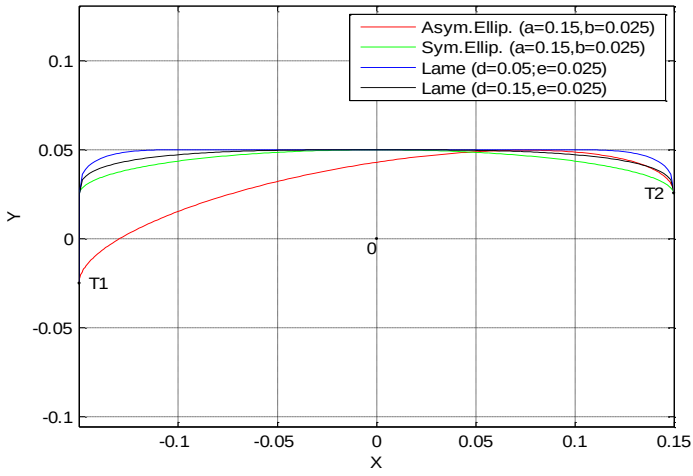

Figure 8: Comparison of the proposed optimal asymmetric bisect elliptical path with the symmetric bisect elliptical path, Lamé curve. (red line: proposed optimal asymmetric bisect elliptical path, green line: symmetric bisect elliptical path, blue line: Lamé curve with d= 0.05 and e= 0.025, black line: Lamé curve with d= 0.15 and e= 0.025).

Figure 8 intuitively demonstrates that the length of the proposed optimal asymmetric bisect elliptical path is smaller than the symmetric bisect elliptical path and Lamé curve-based path, and therefore, the cycle time of pick-and-place operation using the proposed method may be smaller than the other paths. It results in decreasing the cycle period of pick-and-place operation.

Conclusions

In this paper, we proposed an approach for elliptical trajectory planning with vertical straight line segments of pick-and-place robot operation based on radius of curvature, and demonstrated its effectiveness using the simulation.

The process to generate motion profile using the proposed approach consists of the following steps:

(1) Determine optimal angle with minimum length of elliptical path and generate optimal asymmetric bisect elliptical path.
(2) Determine top point and height of the optimal elliptical path with minimum length.
(3) Generate the motion profile suited to geometry of the optimal elliptical path based on curvature radius.

The main conclusions are as follows:

(1) The proposed optimal asymmetric bisected elliptical path has a minimum length, the height of the top point and workspace is smallest than other paths for pick-and-place robot operation.
(2) The proposed motion profile based on radius of curvature of the path is pretty suited to geometry of the optimal elliptical path, and therefore, its velocity, acceleration and jerk are continuous and very smooth, and it enables to smooth the pick-and-place robot operation.
(3) The proposed trajectory planning approach enables to reduce cycle period and ensures smoothness of working action of robot actuators and real-time processing.

The propose trajectory planning approach may be actively used for pick-and-place robot operation under different work conditions.

In this work, we didn't consider the generation of the motion profiles on two vertical straight line segments, and systematic and sufficient analysis about the performance of the proposed trajectory planning method compared with the other previous

methods owing to limited space and time. There is something yet to study. Future work and the next subsequent paper deal with the problems. Future work needs to study more effective method to generate the motion profiles on two vertical straight line segments so that the continuity of the motion velocities satisfy at two tangent points and the motion times during the vertical straight line segments are shortest.

References

1. Javad Jahanpour, Mehdi Motallebi , Mojtaba Porghoveh, A Novel Trajectory Planning Scheme for Parallel Machining Robots Enhanced with NURBS Curves, J Intell Robot Syst. 2016; 82: 257–275.
2. Cesare Rossi, Sergio Savino. Robot trajectory planning by assigning positions and tangential velocities, Robotics and Computer-Integrated Manufacturing. 2013; 29: 139–156.
3. YH Li, T Huang, DG Chetwynd. An approach for smooth trajectory planning of high-speed pick-and-place parallel robots using quintic B-splines, Mechanism and Machine Theory. 2018; 126: 479–490.
4. CM Gosselin, A Hadj-Messaoud. Automatic planning of smooth trajectories for pick-and-place operations, AMSE J. Mech. Des. 1993; 115: 450–456.
5. A Piazzi, A Visioli. Global minimum-jerk trajectory planning of robot manipulators, IEEE Trans. Ind. Electron. 2000; 47.
6. D Constantinescu, EA Croft. Smooth and time-optimal trajectory planning for industrial manipulators along specified paths, J. Rob. Syst. 2000; 17: 233–249.
7. T Chettibi, HE Lehtihet, M Haddad, S Hanchi. Minimum cost trajectory planning for industrial robot, Eur. J. Mech. – A/Solids 2004; 23: 703–715.
8. A Gasparetto, V Zanotto. A new method for smooth trajectory planning of robot manipulators, Mechanism and Machine Theory. 2007; 42: 445–471.
9. A Gasparetto, V Zanotto. A technique for time-jerk optimal planning of robot trajectories, Robot. Comput.-Integr. Manuf. 2008; 24: 415–426.
10. JF Gauthier, J Angeles, S Nokleby. Optimization of a test trajectory for SCARA systems, Adv. Robot Kinemat. Anal.

Des. 2008; 225–234.
11. R Saravanan, S Ramabalan, C Balamurugan. Evolutionary optimal trajectory planning for industrial robot with payload constraints, International Journal of Advanced Manufacturing Technology. 2008; 38: 1213–1226.
12. S Ramabalan, R Saravanan, C Balamurugan. Multi-objective dynamic optimal trajectory planning of robot manipulators in the presence of obstacles, Int J Adv Manuf Technol. 2009; 41: 580–594.
13. A Gasparetto, A Lanzutti, R Vidoni, V Zanotto. Validation of minimum time-jerk algorithms for trajectory planning of industrial robots, ASME J. Mech. Rob. 2011; 3: 031003.
14. HS Liu, XB Lai, WX Wu. Time-optimal and jerk-continuous trajectory planning for robot manipulators with kinematic constraints, Robotics and Computer-Integrated Manufacturing. 2013; 29: 309–317.
15. CD Wang, XJ Wang, H Zheng. Trajectory Planning for a Welding Robot Based on the Bezier Curve, International Journal of Control and Automation. 2015; 8: 351–362.
16. J Jahanpour, M Motallebi, M Porghoveh. A Novel Trajectory Planning Scheme for Parallel Machining Robots Enhanced with NURBS Curves, J Intell Robot Syst. 2016; 82: 257–275.
17. S Kucuk. Optimal trajectory generation algorithm for serial and parallel manipulators, Robotics and Computer–Integrated Manufacturing. 2017; 48: 219–232.
18. RJM Masey, JO Gray, TJ Dodd, DG Caldwell. Elliptical point to point trajectory planning using electronic cam motion profiles for high speed industrial pick and place robots. In: IEEE Conference on Emerging Technologies and Factory Automation (ETFA). Mallorca, Spain, 2009; 1–8. 22-25.
19. GL Wu, SP Bai, P Hjørnet. Parametric Optimal Design of a Parallel Schonflies-motion Robot under Pick-and-place Trajectory Constraints, 2015 IEEE/RSJ International Conference on Intelligent Robots and Systems (IROS) Congress Center Hamburg. Hamburg, Germany. 2015.
20. XQ Zhang, ZF Ming. Trajectory Planning and Optimization for a Par4 Parallel Robot Based on Energy Consumption, Applied Sciences. 2019; 9: 1–19.

21. H Wang, H Wang, JH Huang, B Zhao, L Quan. Smooth point-to-point trajectory planning for industrial robots with kinematical constraints based on high-order polynomial curve. Mech. Mach. Theory. 2019; 139: 284–293.
22. ZJ Wu, JL Chen, TT Bao, JC Wang, LB Zhang, et al. A Novel Point-to-Point Trajectory Planning Algorithm for Industrial Robots Based on a Locally Asymmetrical Jerk Motion Profile. Processes. 2022; 10: 1–18.
23. P Wu, ZY Wang, HX Jing, PF Zhao. Optimal Time-Jerk Trajectory Planning for Delta Parallel Robot Based on Improved Butterfly Optimization Algorithm. Applied Sciences. 2022; 12: 1–22.
24. P Liu, HB Tian, XG Cao, XZ Qiao, L Gong, et al. Pick-and-Place Trajectory Planning and Robust Adaptive Fuzzy Tracking Control for Cable-Based Gangue-Sorting Robots with Model Uncertainties and External Disturbances, Machines. 2022; 10: 1–28.